Eurographics Workshop on Urban Data Modelling and Visualisation (2016)
F. Biljecki and V. Tourre (Editors)

3D Model for Solar Energy Potential on Buildings from Urban LiDAR Data

A. Bill[1], N. Mohajeri[1*], J.-L. Scartezzini[1]

[1] Solar Energy and Building Physics Laboratory (LESO-PB), Ecole Polytechnique Fédérale de Lausanne (EPFL), Switzerland.
[*] To whom the correspondence should be addressed. E-mail: nahid.mohajeri@epfl.ch

Abstract

One of the most promising sustainable energies that can be considered in urban environments is solar energy. A 3D model for solar energy potential on building envelopes based on urban LiDAR data was developed in this study. The developed algorithm can be used to model solar irradiation with high spatio-temporal resolution for roof-, facade-, and ground surfaces simultaneously, while taking into account the surrounding vegetation. Global solar irradiation is obtained for regularly spaced points on building- and ground surfaces with a spatial resolution of 1m^2 and a time resolution of 1 hour. The algorithm has been implemented in Matlab and results were generated for two different test areas in the city of Geneva, Switzerland. The results for these specific areas show that, even in a dense urban area, the upper parts of south-east to south-west oriented facades receive 600 to 1000 kWh/m^2/year of solar input, which is suitable for active solar installations. The results also show that south oriented facades can get higher solar input during winter months than the low inclined roof surfaces. This demonstrates that, depending on the latitude, facades can have a significant impact on the solar potential of buildings in urban areas, particularly for a sustainable energy planning application.

Categories and Subject Descriptors (according to ACM CCS): I.3.3 [Computer Graphics]: Picture/Image Generation—Line and curve generation

1. Introduction

Urban areas in many countries offer great opportunities for on-site solar energy production, thereby minimising the loss or transformation through energy transmission. Photovoltaic (PV) technology is one of the most promising emerging technologies for deployment of solar energy in urban areas. While it is estimated that building facades represent 60% to 80% of building surfaces [EFPT14], many studies focus on modelling solar energy potential on roofs from building to neighbourhood and urban scale (e.g. [SAD*12], [PL13]). Several methods/tools have been used to assess the solar energy potential for building rooftops. The tools include the ArcGIS Solar Analyst [FR99], the GRASS r.sun [HS*02], CitySim [KMB*10], [MUG*16] or the RADIANCE lighting simulation software [Mon10]. Also, several studies use statistical methods, aerial images and ArcGIS software using LiDAR data, as well as data-driven approaches (Support Vector Machine) to determine roof geometries and associated roof areas to estimate the PV potential at urban scale [Mon10], [AMS15]. Very few studies, however, explore modelling urban scale solar energy potential for building facades [RCBG11]. CitySim, a software that has been developed at Solar Energy and Building Physics Laboratory at EPFL, uses vector building data to simulate solar irradiation on building envelopes including facades [KMB*10], [MUG*16]. The CitySim software computes solar irradiation very precisely, considering also the physical characteristics of buildings as well as reflected radiation. Nevertheless, its performance and precision relies on the underlying vector layer which is time-consuming to produce and seldom exists for large urban areas. Raster-based models using point data collected by LiDAR technology can be a suitable alternative for modelling solar potential on facades [RCBG11], [RCB13], [CRPB14]. One important advantage of using 3D LiDAR data is that buildings, their geometry and the urban surroundings can be interpolated from point data. Carneiro et al. in 2009 propose a method combining LiDAR point data and building footprint vector layers to assess the solar potential on facades [CMD09]. The results of this study show that, while the accuracy of the 3D building model is promising, the resolution used for the computation of solar irradiation on facades needs improvement. In addition, in this method the vegetation and other obstacles from building surroundings are not considered. A recent study by several researchers from the university of Lisbon [RCB13] uses high resolution airborne LiDAR point data (average density of 20 points per m^2) for solar facade modelling. The results have been published in several journals [RCBG11], [RCB13], [CRPB14]. We applied a similar approach as was used in [RCBG11], [RCB13], [CRPB14] but improved the model precision and computation time, using LiDAR point data from a neighbourhood in the city of Geneva in Switzer-

DOI: 10.2312/udmv.20161420

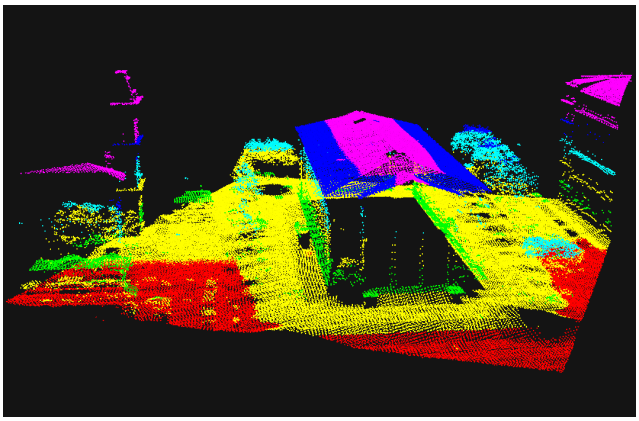

Figure 1: *Visualisation of LiDAR data. The variation in colours shows the differences in elevation values for points and surfaces*

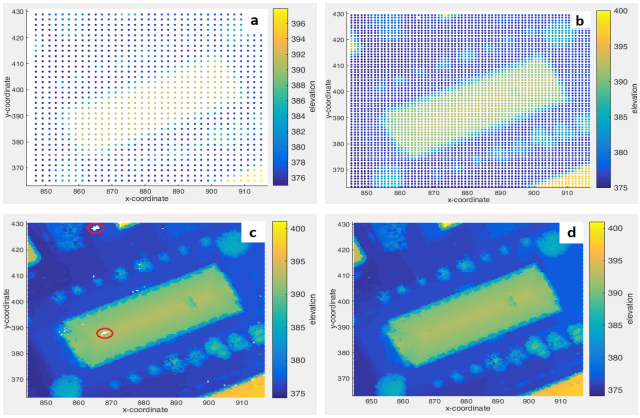

Figure 2: *DEM interpolation for different spatial resolutions. (a) cell size = 2m*2m, (b) cellsize = 1m*1m, (c) cellsize = 0.5m*0.5m, (d) Interpolation of missing pixel values*

land. Thus, the main aim of this study is to develop an algorithm based on urban LiDAR point data to model solar irradiation not only on facades but also on building roofs and ground surfaces.

2. Data and test areas

We use high resolution urban LiDAR point data which is available for the whole canton of Geneva (administrative division in Switzerland) and can be collected for free from *Le système d'information du territoire à Genève (http://ge.ch/sitg/)*. The LiDAR point data for Geneva was created in 2013 and has the following characteristics: Average point density 15 points/m^2, vertical precision $\pm$10cm and horizontal precision $\pm$20cm. While these data points represent the urban form (building geometry, trees and landscape) precisely, they have some limitations. For example, there are nearly no points with the same X and Y coordinates which makes it difficult to map features like building facades. The visualization of LiDAR point data for one building and its surrounding environment is presented in Fig. 1. Weather conditions have large impacts on the results of modelling solar irradiation. We use hourly measured weather data from Meteonorm, which includes direct and diffuse solar irradiation on horizontal surfaces. The data presents averaged irradiation values for the years 1991 to 2010. While the historical weather data is quite useful for monthly and yearly solar irradiation estimation, for short term variability (e.g. hourly estimation) it would be favourable to use a statistical model (e.g. markov chain). However, in this study we use the averaged weather data from Meteonorm. We have selected two test areas: (a) consists of one building with the surrounding environment (total considered area 5'250m^2) to test the developed algorithm. The selected building is located in the Jonction neighbourhood in the city of Geneva. It is shown in Fig. 1. (b) consists of several buildings (total considered area 113'800m^2) from the same neighbourhood. It is used to analyze the results. The second test area includes buildings with different configurations (e.g. courtyard, building block) and roof types (e.g. flat, slightly to moderately sloped).

3. Methodology

Below we explain in different steps how the algorithm for spatio-temporal solar irradiation modelling using LiDAR point data has been developed.

3.1. Elevation raster computation

The LiDAR point data is interpolated to a DEM raster with a suitable cell size for computation. As mentioned, the average point density for the original data is 15 points per m^2. While it is crucial to have such a high resolution for an accurate description of the urban landscape, the computational effort to treat such a huge number of points is very high. In the following we explain how we reduce the number of points without losing much accuracy. After the LiDAR point file is imported in Matlab, a spatial resolution is defined which will be used as pixel size for the resampling of the data. A regular grid is defined based on the selected resolution and for every cell of this grid the corresponding points from the LiDAR point file are selected. There are, however, outlier points (e.g. due to reflections of laser from birds) which should be removed. We use the elevation (z-value) of the points in order to identify such outliers. If the z-value of a point is more than 20m away from the average z-value of all points located in a given cell, it will be deleted. The z-value of the corresponding cell is then set to the average of the remaining points. The result of this operation is shown in Fig. 2 for different spatial resolutions (a to c). As can be seen in the figure the details become clearer when the cellsize decreases. However, the number of missing pixel-values also increases with decreasing cellsize (white spots marked in red circles in Fig. 2c). We identify the missing pixels and use the values of the neighbouring cells in order to interpolate an appropriate z-value. The result of this interpolation for a resolution of 0.5m by 0.5m is shown in Fig. 2d. Another important factor is computational time. For the area shown in the figure the computation takes 2.6 seconds using a resolution of 1m by 1m. However, if the resolution is set to 0.5m by 0.5m the computation time increases to 9.5 seconds. In addition, a smaller resolution will also augment the number of created cells which will increase the computation time of further steps. When

the resolution is set to 1m by 1m the number of cells generated for this test area is 5'250. Applying a resolution of 0.5m by 0.5m results in a fourfold increase of generated points. In order to stay within reasonable computation time, the spatial resolution used for this study is set to 1m by 1m. This resolution is considered to be satisfactory for the purposes of the proposed model.

3.2. Extrapolation of elevation raster to regular 3D grid

The DEM raster created in step 1 gives useful information about the topography of the features in the site. However, it does not show the information related to the vertical surfaces (e.g. building facades). In step 2, we extrapolate the two dimensional raster, which stores the site information as pixel values, into a 3 dimensional grid. For ground and roof surfaces this can be easily done by considering the pixel value as z-coordinate. The challenge is to identify those pixels that correspond to facades and extend them so as to create hyperpoints (i.e. a series of points with equal x and y-coordinates but different z-values). We use similar assumptions as reported in Redveik et al. 2013 [CRPB14] where it is estimated that DEM pixels with slope values greater than 72 degrees most probably correspond to building facades. The following steps show the process:

- Compute slope and aspect values for each point
- Create hyperpoints where the slope values of the original points are larger than 72 degrees
- Improve the facade model including (a) remove redundant hyperpoints, (b) adjust height of hyperpoints
- Remediate high slope values close to facades

Compute slope and aspect values for each point:
We used a 3x3 pixel moving window for the estimation of slope and aspect values. The applied computations are equivalent to the method which is used in ArcGIS for the creation of slope and aspect maps. The results are visualized in Fig. 3.

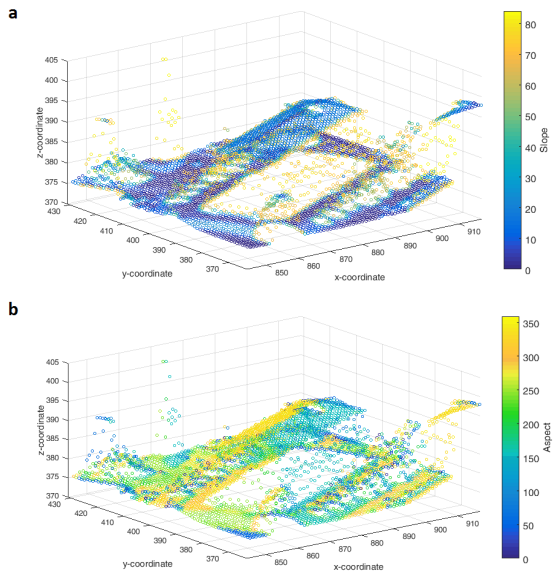

Figure 3: *Results for (a) slope and (b) aspect computation*

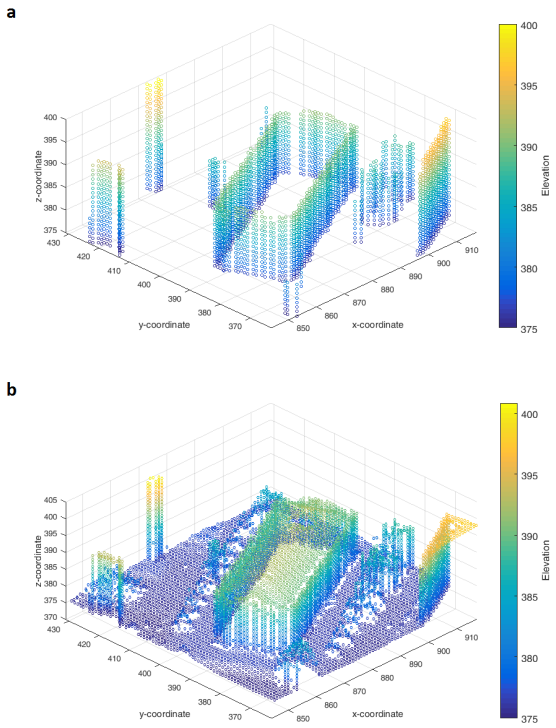

Figure 4: *Results from the hyperpoint creation: (a) produced hyperpoints, (b) complete 3D grid*

Create hyperpoints where the slope values of the original points are larger than 72 degrees:
We use two criteria in order to add the hyperpoints: (1) identify points with a slope larger than 72 degrees, (2) identify the points for which the difference between the cells own z-value and both the lowest and highest neighbour is more than 3m. The second criteria is necessary in order to eliminate points which are located on the edge of a roof or close to the facade on the ground. These points often get high slope values assigned although they are not actually located on a facade. This happens when one or several of their neighbouring cells are located on a facade and, thus, have much lower or much higher z-values. If both conditions are fulfilled, hyperpoints are added with identical x- and y-coordinates and z-values that vary from the elevation of the lowest neighbour to the highest neighbour while keeping all spatial resolutions similar. The results are visualized in Fig. 4.

Improve the facade model including (a) remove redundant hyperpoints, (b) adjust height of hyperpoints:
While the results shown above are promising, several problems remain. (a) There are redundant hyperpoints which can become a problem during the computation of solar irradiation as some of these facade points would shade those behind them. In addition, the computation time increases with the number of points which is another reason why these redundant hyperpoints should be removed. The method used to identify such hyperpoints is based on the assumption that, if parallel hyperpoints exist, only the "largest"

ones should be kept, while those which are at least 3m shorter than their largest neighbour are discarded. The value 3 meters was chosen based on different test runs and the comparison of the results. (b) Another improvement can be made concerning the height of hyperpoints. Since a facade generally has a constant height, the small irregularities in height of neighbouring hyperpoints should be corrected.

Remediate high slope values close to facades:
We select all roof- and ground points which are up to two units away from a remaining hyperpoint. The new slope value assigned to all selected roof cells is the minimum slope value of the selected roof cells. For ground cells it is the minimum slope value of the selected ground cells. The margins have been chosen by analyzing the result of test runs with different margin values. The results are shown in Fig. 5.

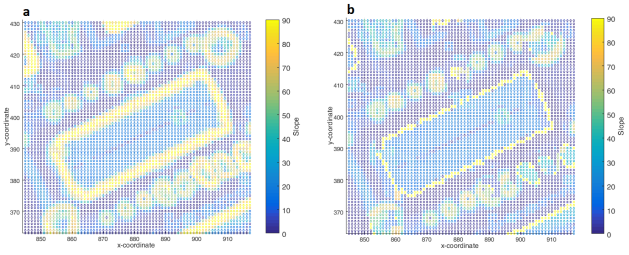

Figure 5: *Slope-maps before (a) and after (b) remediation of biased values*

3.3. Solar irradiation matrix computation

To compute the solar irradiation matrix, the following steps need to be taken: (a) computation of the suns position for every hour of the considered time interval, (b) transformation of direct horizontal irradiation to direct irradiation on inclined planes for every combination of slope and aspect values and every hour of the considered time interval, (c) transformation of diffusive horizontal irradiation to diffusive irradiation on inclined planes for every combination of slope and aspect values and every hour of the considered time interval. For the computation of the suns position (azimuth and elevation angle of the sun for every hour), we implemented the Sun-Position Algorithm in Matlab which is proposed by Blanco-Muriel et al., 2001 [BMAPLMLC01]. The calculation of direct solar irradiation on inclined planes is purely geometrical and the model described in Gulin et al., 2013 [GVB13] is used. An anisotropic model described by Klucher, 1979 [Klu79] is used to calculate the diffuse solar irradiation on inclined planes. The results for global annual solar irradiation as a function of aspect and slope are displayed in Fig 6. It can be seen from the figure that the highest annual solar input in Geneva is received by south-west oriented surfaces with slope values between 30 and 60 degrees inclination. The local weather conditions in Geneva seem to be more favourable in the afternoon than in the morning which would explain these results. The mornings are often foggy in the city of Geneva, as a result the irradiation values on the east to southeast oriented surfaces are affected. The suns position is lower in the afternoon; therefore, higher slopes with south-west aspect

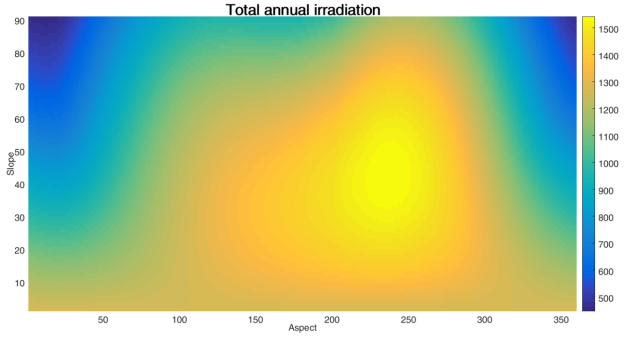

Figure 6: *Annual solar irradiation, kWh/m^2/year, as a function of aspect and slope*

reach the highest annual irradiation values. Another interesting finding is that for well exposed surfaces (not much in shadow) even north-oriented surfaces with slopes up to 20 degrees can reach annual solar irradiation values above 1000 kWh/m^2. The same is true for facades with aspects from southeast to west. The deployment of solar PV can be economically favourable starting from annual irradiation levels of 800kWh/m^2 and for solar thermal applications this value can even drop to 600kWh/m^2 [CMD09]. This shows that the active use of solar energy on well exposed facades has great potential in Switzerland.

3.4. Shadow algorithm / viewshed computation

A crucial part of the solar irradiation model is the consideration of shadows from surrounding elements. Thus, we compute a viewshed for each point in the considered area. This is done by identifying, for a given point, the largest elevation angle corresponding to an object in sight of this point in N azimuth directions. The discrete set of azimuth and elevation angles for each point can then be used for both the computation of the sky view factor (fraction of the sky visible to a given point) and the determination of whether or not the sun is visible at a certain time. Fig. 7 shows the results for one point of the test area located on a facade.

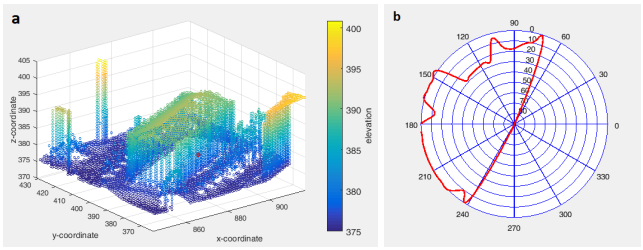

Figure 7: *Example of viewshed result (b) for one particular point on a facade (a)*

3.5. Direct and diffusive irradiation on every point

After computing the solar irradiation matrix and the viewshed, the direct and diffusive solar irradiation can be calculated. This is done

in two different steps, as the influence of the viewshed is different for direct and diffusive irradiation. Direct irradiation is calculated based on the multiplication of two vectors. (a) The first vector can be computed by comparing the elevation angle of the suns position for every hour of the considered time period with the elevation angle from the viewshed which corresponds to the sun's azimuth angle. If the suns elevation angle is larger than the one of the viewshed, the sun is visible during the corresponding hour and the value is set to 1. If not, there is an obstacle shading the point of interest and the value is set to 0. (b) A second vector is produced from the direct irradiation matrix. More specifically, the elements for every considered hour which correspond to the slope and aspect values of the point for which irradiation is computed are extracted. The two vectors (direct irradiation vector and binary shadow vector) are then multiplied element per element. The so obtained final vector contains the direct irradiation values for the point in question with hourly resolution. For the computation of diffuse solar irradiation a vector containing the diffusive irradiation values for every considered hour is produced from the diffuse irradiation matrix. This vector is then multiplied with the sky view factor which is computed based on the viewshed of a given point.

4. Results

The developed algorithm was applied to the larger test area briefly described in section 2. Annual, monthly, daily, and hourly solar irradiation on roof-, facade-, and ground surfaces were computed for the case study. The results of annual solar irradiation are shown in Fig. 8. The values obtained for roof-, façade- and ground surfaces vary from 3 to 1524 kWh/m^2/year. Values for points located on the lower parts of facades are generally very low since they receive almost no direct and only very little diffuse irradiation. This is more common in the dense areas. It is to be noted here that reflected radiation is not considered by the model which explains the surprisingly low values. The values computed for upper parts of south-east to south-west facing facades are as high as 700kWh/m^2/year in the dense areas and up to 1000kWh/m^2/year for the less dense areas. The irradiation values on most roof points are computed between 900kWh/m^2/year and 1300kWh/m^2/year. Annual solar irradiation profiles for two different points located on the roof and facade of a building have been generated in Fig. 9 using a daily resolution. The first point, which is located on the roof and facing south-east, receives around 1250 kWh/m^2/year of solar energy input. The second point is located just below the roof point on the facade facing the same direction. It receives only 600-700kWh/m^2/year of global annual solar irradiation. The irradiation profiles for roof and facade (Fig. 9) show that, although the difference of solar irradiation during the summer months is very high, which explains why the global annual irradiation is almost twice as high for the roof point, the difference during the winter half-year is much lower. On some days in January and December the potential for facades actually exceeds the one for roofs. We compared the results of the LiDAR-based 3D model developed in this study with the roof solar raster models generated from http://ge.ch/sitg/. We found that of all roof surfaces larger than $10m^2$ and for which both models estimate similar slope values ($\pm 25°$), 90% reach values between -20% and +30% compared to the SITG model. There are, however, several differences in the assumptions of the two models which all affect the results. (a) The SITG model uses averaged irradiation data for the years 1980-2000 while our model considers the data for 1991-2010. (b) SITG uses a model for isotropic diffuse radiation while we use an anisotropic model. (c) There are some differences in the estimated slope values of roof surfaces due to the remediation of high slope values on roof edges considered in our model. In order to produce a more accurate validation of the proposed model, comparisons of facade- and roof solar irradiation with vector-based models (e.g. CitySim) will be one of the future expansions of this study.

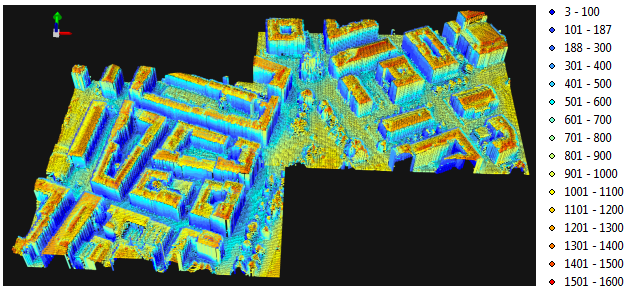

Figure 8: *Results for annual solar irradiation (kWh/m^2)*

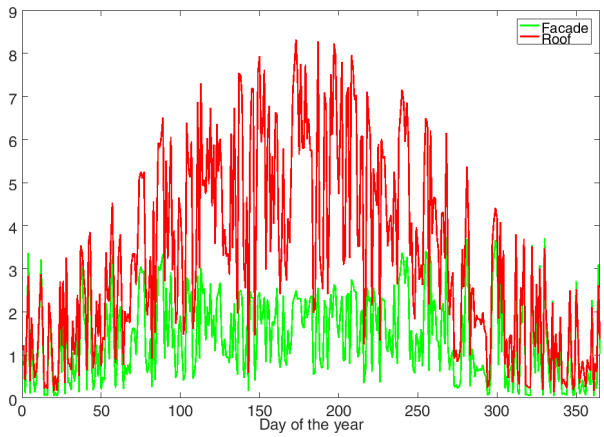

Figure 9: *Daily solar irradiation (kWh/m^2) profiles for roof and facade points with identical azimuth*

5. Discussion and conclusion

A 3D solar irradiation algorithm for modelling building roof-, facade- and ground surfaces using urban LiDAR point data has been developed in this study. The algorithm has been implemented in Matlab and results were generated for two different test areas in the city of Geneva in Switzerland. The method is entirely based on LiDAR point data and uses a spatial resolution of 1m^2 and a time resolution of 1 hour. The developed 3D solar algorithm has several advantages in comparison with the algorithm implemented for 2D solar raster computation in ArcGIS: (a) high slope values close to facades are corrected before solar irradiation is computed, (b) the possibility of using measured weather data, (c) the possibility of using an anisotropic- instead of an isotropic model for diffuse

irradiation, (d) more accurate computation of solar irradiation values on an hourly bases for every output interval. In addition, the developed algorithm has several advantages compared to vector-based solar models: (a) no need to produce building geometry in advance, (b) automatically considering topography and urban landscape using LiDAR data, (c) LiDAR data is often freely available and easy to use. However, there are also some limitations, partly due to the use of point data, partly because of some limitations of the algorithm which need to be addressed in further developments. (a) The use of airborne LiDAR point data allows for quite accurate interpolations of the urban landscape. However, it is not possible to consider features such as balconies, window frames or overhanging roofs, which can have an important influence on the solar potential of a facade. (b) Reflected radiation is not considered by the model which leads to an important underestimation of the irradiation received in urban valleys. (c) The criteria for the outlier identification in section 3.1, as well as the removing of redundant hyperpoints in section 3.2 have been determined by testing for best performance based on the test areas. They are likely to work as intended for cities with similar characteristics than Geneva (rather low buildings), however, they probably will fail when applied in cities like New York. (d) The accuracy of the viewshed computation (section 3.4) depends on the spatial resolution of the grid. The obstacles that obstruct the sky for a given point are often close by. Respective to the point of interest, two adjacent points corresponding to a close by object are, however, located at different azimuth angles. If the spatial resolution is to coarse for the chosen viewshed resolution, it can happen that an obstacle, e.g. an opposite facade, is not represented as a continuous object in the resulting viewshed. This results in an over estimation of the irradiation values. (e) The viewshed computation is very time consuming and slows the algorithm considerably down. The computation time could be reduced by only considering the surroundings of a given point up to a specified perimeter. However, this would again raise issues if applied in cities with very large buildings, such as New York. The results presented in the previous section show that for a city like Geneva, located at a latitude of 46° N, facades can have an important potential for active solar installations. During the winter months these building surfaces can, in some cases, even compete with roof surfaces. This effect is highly dependent on the location of a building. Around the equator and in low latitudes, roof surfaces will always have much higher potentials as the sun passes at high elevation angles throughout the whole year. In mid-latitudes, however, we can observe important differences in summer but similar potentials for winter months due to the lower solar course during this time of the year. Moving to higher latitudes the solar potential of facades relative to the potential of all building surfaces becomes more important. Therefore, 3D solar models including facades are particularly interesting for sustainable energy planning applications at urban scale in mid- to high latitude countries. After some further developments, including the remediation of the above mentioned limitations of the algorithm as well as testing on areas with different urban characteristics, the algorithm developed in this study could be implemented in a software like ArcGIS in order to provide users with a simple tool for the generation of 3D solar irradiation maps.

References

[AMS15] ASSOULINE D., MOHAJERI N., SCARTEZZINI J.-L.: A machine learning methodology for estimating roof-top photovoltaic solar energy potential in switzerland. In *Proceedings of International Conference CISBAT 2015 Future Buildings and Districts Sustainability from Nano to Urban Scale* (2015), no. EPFL-CONF-213375, LESO-PB, EPFL, pp. 555–560. 1

[BMAPLMLC01] BLANCO-MURIEL M., ALARCÓN-PADILLA D. C., LÓPEZ-MORATALLA T., LARA-COIRA M.: Computing the solar vector. *Solar Energy 70*, 5 (2001), 431–441. 4

[CMD09] CARNEIRO C., MORELLO E., DESTHIEUX G.: Assessment of solar irradiance on the urban fabric for the production of renewable energy using lidar data and image processing techniques. In *Advances in GIScience*. Springer, 2009, pp. 83–112. 1, 4

[CRPB14] CATITA C., REDWEIK P., PEREIRA J., BRITO M. C.: Extending solar potential analysis in buildings to vertical facades. *Computers & Geosciences 66* (2014), 1–12. 1, 3

[EFPT14] ESCLAPÉS J., FERREIRO I., PIERA J., TELLER J.: A method to evaluate the adaptability of photovoltaic energy on urban façades. *Solar Energy 105* (2014), 414–427. 1

[FR99] FU P., RICH P. M.: Design and implementation of the solar analyst: an arcview extension for modeling solar radiation at landscape scales. In *Proceedings of the Nineteenth Annual ESRI User Conference* (1999), vol. 1, pp. 1–31. 1

[GVB13] GULIN M., VAŠAK M., BAOTIC M.: Estimation of the global solar irradiance on tilted surfaces. In *17th International Conference on Electrical Drives and Power Electronics (EDPE 2013)* (2013), pp. 334–339. 4

[HS*02] HOFIERKA J., SURI M., ET AL.: The solar radiation model for open source gis: implementation and applications. In *Proceedings of the Open source GIS-GRASS users conference* (2002), vol. 2002, pp. 51–70. 1

[Klu79] KLUCHER T. M.: Evaluation of models to predict insolation on tilted surfaces. *Solar energy 23*, 2 (1979), 111–114. 4

[KMB*10] KÄMPF J. H., MONTAVON M., BUNYESC J., BOLLIGER R., ROBINSON D.: Optimisation of buildingsâĂŹ solar irradiation availability. *Solar energy 84*, 4 (2010), 596–603. 1

[Mon10] MONTAVON M.: Optimisation of urban form by the evaluation of the solar potential. 1

[MUG*16] MOHAJERI N., UPADHYAY G., GUDMUNDSSON A., ASSOULINE D., KÄMPF J., SCARTEZZINI J.-L.: Effects of urban compactness on solar energy potential. *Renewable Energy 93* (2016), 469–482. 1

[PL13] PENG J., LU L.: Investigation on the development potential of rooftop pv system in hong kong and its environmental benefits. *Renewable and Sustainable Energy Reviews 27* (2013), 149–162. 1

[RCB13] REDWEIK P., CATITA C., BRITO M.: Solar energy potential on roofs and facades in an urban landscape. *Solar Energy 97* (2013), 332–341. 1

[RCBG11] REDWEIK P., CATITA C., BRITO M., GRANDE C.: 3d local scale solar radiation model based on urban lidar data. In *Proceedings of the ISPRS Workshop High-Resolution Earth Imaging for Geospatial Information, Hannover, Germany* (2011), Citeseer, pp. 14–17. 1

[SAD*12] STRZALKA A., ALAM N., DUMINIL E., COORS V., EICKER U.: Large scale integration of photovoltaics in cities. *Applied Energy 93* (2012), 413–421. 1